J. Phys. Soc. Jpn, 78 (2009) 104301 ©*The Physical Society of Japan*

Suppression Mechanism of Electron Emission under Fast Cluster Impact on Solids

Hideyuki ARAI[1], Hiroshi KUDO[1,2]*, Shigeo TOMITA[1], and Satoshi ISHII[2]

[1]*Institute of Applied Physics, University of Tsukuba, Ibaraki 305-8573, Japan*
[2]*UTTAC, University of Tsukuba, Ibaraki 305-8577, Japan*

We have specified the mechanism of suppressed electron emission from surfaces bombarded by fast cluster ions. From key information obtained from a comparison of the electron emissions for insulator KCl and conductor graphite, we concluded that the suppression is predominantly caused by the disturbance of the electron transport by the electric potential generated by moving cluster atoms. The possible shift from suppressed emission to enhanced emission of electrons as cluster speed increases is also discussed in relation to that in the case of cluster stopping power.

KEYWORDS: cluster beam, cluster impact, electron emission

1. Introduction

The electronic interaction of fast atom clusters with solids has been studied in two main categories that are closely related to each other, i.e., stopping power and electron emission.[1] The vicinage effect on cluster stopping power has been approached in terms of the dielectric response.[2–4] In contrast, the mechanism of the vicinage effect on electron emission has not been specified yet.[5] The pronounced suppression of electron emission has been observed for bombardment by clusters of up to ∼100 keV/u, beyond which cluster beams are unavailable at present, except for hydrogen clusters. Note that the thus-far-proposed mechanisms of suppressed emission, for example, reduced charge states, a sweeping-out-electron effect, and molecular orbitals, are concerned with the production stage of electrons.

Recently, the energy spectra of electrons induced by fast clusters have been measured at 9–42 keV/u mainly using C_n^+ ($n \leq 8$).[6,7] As a notable phenomenon, the convoy electron yield at ∼23 eV (corresponding to the projectile velocity) is proportional to the cluster size n. Since convoy electron yield should be proportional to the density of scattered electrons around the projectiles, the observed n dependence implies that the primary electrons scattered by the projectiles effectively suffer no vicinage effect. An important conclusion deduced from these studies is that the main mechanism of suppressed emission is not in the production stage, but in the stages of transport or surface transmission.

*e-mail address: kudo@bk.tsukuba.ac.jp

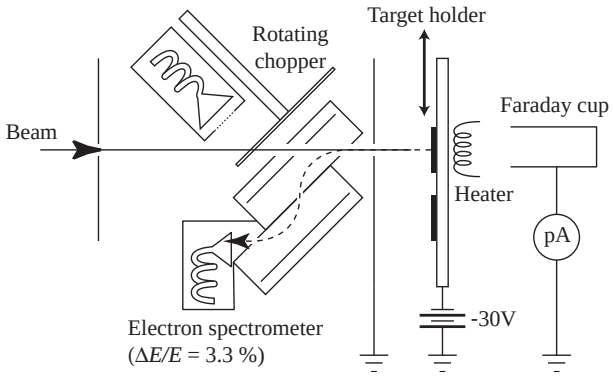

Fig. 1. Schematic drawing of the experimental setup.

Furthermore, suppressed electron emission was observed at electron energies lower than 10 eV at 180°, while at 0° the suppression is extended up to ∼100 eV. No essential difference was observed between the n dependences of the electron suppression for the emission of low-energy electrons in two directions. The suppression at 0° was recognized for a thick carbon foil target for which the estimated atomic spacing of the transmitted cluster atoms is as wide as ∼10 Å, implying the existence of long-range interaction.

To specify the mechanism of interest, an effective approach might be the analysis of the observed n dependence of electron yield. In the present work, experimental data are collected extensively for the insulator KCl. Data for KCl should include key information on the mechanism of suppressed electron emission. For alkali halides, we may expect that the electron yield is higher than that for typical conductors by a factor of ∼10,[1] which definitely affects the surface transmission stage of electron emission. Moreover, electron emission from KCl is affected by track potential,[8,9] which is one of the possible mechanisms of suppressed electron emission.

2. Experimental Methods

Figure 1 shows a schematic drawing of the experimental setup, which is similar to that used in a previous study,[6] except for the beam chopper system adopted in the present experiments for monitoring weak beam current. C_n^+ beams of 12.5 and 41.7 keV/u (0.15 and 0.50 MeV/atom, respectively) were obtained from the 1 MV Tandetron accelerator at the University of Tsukuba. Cluster ions from the accelerator passed through an aperture of 1 mm diameter and impinged on KCl(001) or highly oriented pyrolytic graphite (HOPG), which were cleaved in air. The beam direction was chosen to avoid the channeling effect. The target holder on which the samples were mounted was kept at 220 °C during the experiments. The heating effectively prevented the KCl surface from macroscopic electrical charging.[8]

Electrons emitted from the sample biased at −30 V are accelerated to the grounded plate placed about 1 cm upstream from the target, so that the emitted electrons at 180° are ac-

celerated and detected by the electron spectrometer. Such preacceleration enables the improvement in the transmission efficiency of low-energy electrons through the spectrometer. The energy resolution of the spectrometer is 3%, and therefore, the present energy resolution (i.e., the energy acceptance of the spectrometer) ΔE at the electron energy E [eV] is given by $\Delta E = 0.03(E + 30)$ [eV]. More details of the electron measurement are given elsewhere.[6,7]

To monitor the beam current on the order of ∼0.1 pA required in the present measurements, we adopted a beam-chopper system using particle-induced electron emission. The chopper of an aluminum disc with twelve 15°–wide slits was motor-driven at about 180 rpm under a pressure of $\sim 3 \times 10^{-6}$ Pa through a magnet-coupled vacuum feedthrough. The frequency of chopping was much higher than that of the fluctuation in beam intensity. The electrons emitted from the chopper were measured using an electron multiplier placed ∼25 mm from the chopper. The grid in front of the electron multiplier was biased at −100 V so that only high-energy electrons were measured, whose counts were proportional to the number of atoms incident on the target. Note that negative voltage was adjusted so that the count rates were in an adequate range, i.e., 10^3–10^4 counts/s.

3. Results and Discussion

3.1 Linear n dependence of electron yield

Figures 2 and 3 show the energy spectra of electrons for KCl and HOPG bombarded by C^+ of 12.5 and 41.7 keV/u, respectively. The yields are plotted for the same number of incident ions. The emitted electrons are accelerated by the target voltage (−30 V), and therefore, the real zero-energy corresponds to 30 eV on the horizontal axes of Figs. 2 and 3. For a measured energy spectrum, the integrated yield Y_n per n–atom cluster is given by the area under the spectrum, taking into account the energy dependence of the energy acceptance ΔE, noted in §2. We see that Y_1 for KCl is higher than that for HOPG by factors of 9 and 7 for 12.5 and 41.7 keV/u, respectively. Also, the peak energy for KCl is lower than that for HOPG by ∼1 eV. Such differences of alkali halides from conductors are consistent with the results of the experiments by König and coworkers, in which inert gas ion beams with energies below 30 keV were used.[1,10]

The ratio of the integrated yield, Y_n/Y_1, is shown as a function of n in Figs. 4 and 5 for 12.5 and 41.7 keV/u, respectively. Suppressed electron emission, i.e., $Y_n/Y_1 < n$, is clearly seen. Furthermore, the n dependences of Y_n/Y_1 for KCl and HOPG are very similar, although Y_1 is different from each other by a factor of ∼10 (Figs. 2 and 3). The difference between the two targets is much smaller than that in the case of suppression from $Y_n/Y_1 = n$. These results provide important information on the possible effects associated with the surface transmission of electrons, and with track potential.

The surface bombarded by a fast ion is positively charged by electron emission, although the charged region quickly recovers its neutral charge. The widely charged surface due to

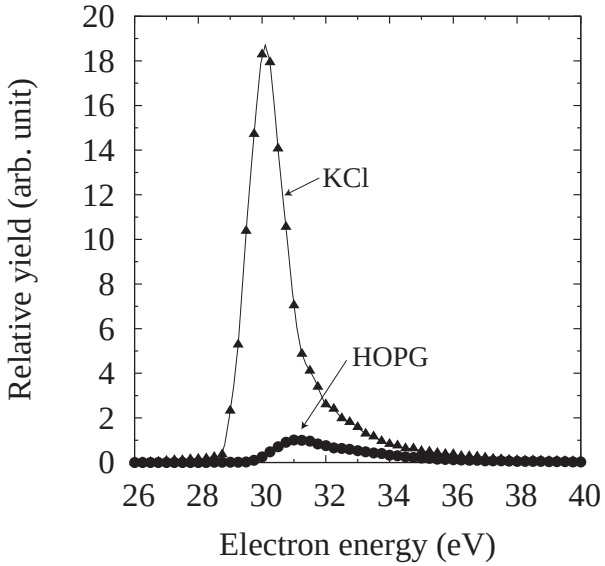

Fig. 2. Energy spectra of electrons emitted from KCl and HOPG bombarded by C_1^+ of 12.5 keV/u (0.15 MeV/atom). Note that the real zero-energy corresponds to 30 eV on the horizontal axis (see text). The yields are shown for the same number of incident C atoms.

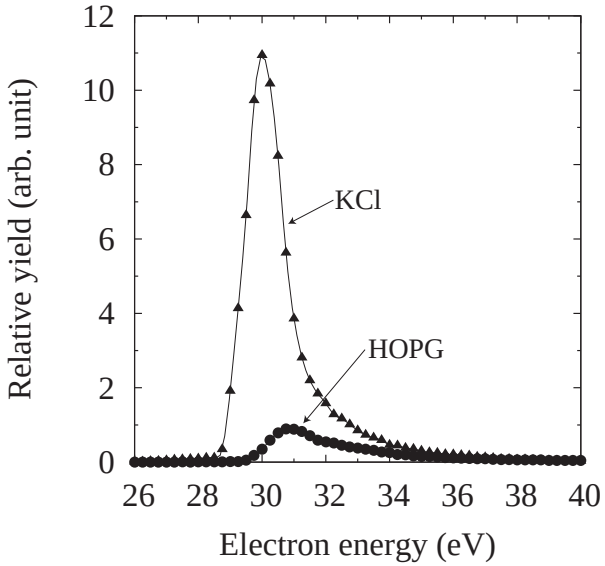

Fig. 3. Energy spectra of electrons for 41.7 keV/u (0.50 MeV/atom) C_1^+, shown similarly to Fig. 2.

cluster bombardment might disturb the surface transmission of outgoing electrons, which leads to the suppressed emission of electrons. Such a process for KCl must be more pronounced than that for HOPG because of the number of emitted electrons larger in the former than in the latter by a factor of ∼10, which gives rise to a higher surface barrier by a factor of ∼10, and because of the slower recovery of the charged surface. However, the similarity of the Y_n/Y_1

vs. n plots for KCl and HOPG indicates that surface transmission is not the main factor for suppressed electron emission. Probably, the recovery of the charged surface is so fast that the effect of surface charging becomes much smaller than that of the electron suppression of interest.

Kimura and coworkers reported that the reduced electron emission from a KCl surface bombarded grazingly by 0.5 MeV/u light ions can be explained by the track potential induced on the surface.[8,9] In the present experiments, accordingly, we may expect multiple track potentials along each of the cluster atoms in KCl. In this case, the produced electrons can be captured by the track potential of neighboring cluster atoms, which should cause a stronger suppression of electron emission than that in the case of the conductor HOPG, in which there is no effective track potential. The small difference observed between the Y_n/Y_1 vs n plots for KCl and HOPG demonstrates that track potential is only a minor factor for suppressed electron emission.

As is seen in Figs. 4 and 5, the n dependence of Y_n/Y_1 can be expressed empirically as

$$Y_{\mathrm{n}}/Y_1 = 1 + \alpha\,(n-1)\ , \tag{1}$$

where α is a constant.[6] α is also the saturation value of the yield per atom, Y_{n}/nY_1, as n increases.[11] Such a linear n dependence also holds for the experimental data reported so far. The values of α for available experimental data are summarized in Table I. They are typically in the range $0.3 < \alpha < 0.7$. It is also recognized that for a given combination of the target and ion species, α increases, i.e., the extent of suppression decreases, with increasing ion velocity.

Note that the parameter α in eq. (1) can be determined uniquely in the case of a dicluster ($n = 2$). This means that the fundamental process of the vicinage effect for $n > 2$ must be the same as that for $n = 2$. The vicinage effect for $n = 2$ results from the interaction of electrons generated by a cluster atom with another atom. Essentially the same interaction exists even for $n > 2$ under a limited condition. A fast cluster of n atoms can be obtained by adding an atom virtually to a fast cluster of $n - 1$ atoms. In this procedure, Y_n/Y_1 is increased by the amount of α, in accordance with eq. (1), only when the vicinage interaction originates effectively from the new pair of atoms. Surely, these atoms are the added atom and the nearest one of the $n - 1$ cluster atoms.

3.2 Electric potential generated by a moving ion

Since surface transmission is not an important factor for suppressed electron emission for cluster bombardment, as mentioned in §3.1, the suppression mechanism of interest is in the transport stage of electrons. Moreover, the possible reduced transport by track potential has also been excluded from the experimental results for KCl.

The origin of the interaction is probably the electric potential generated by a moving cluster atom in the target. The Coulomb field of the moving atom polarizes the electron

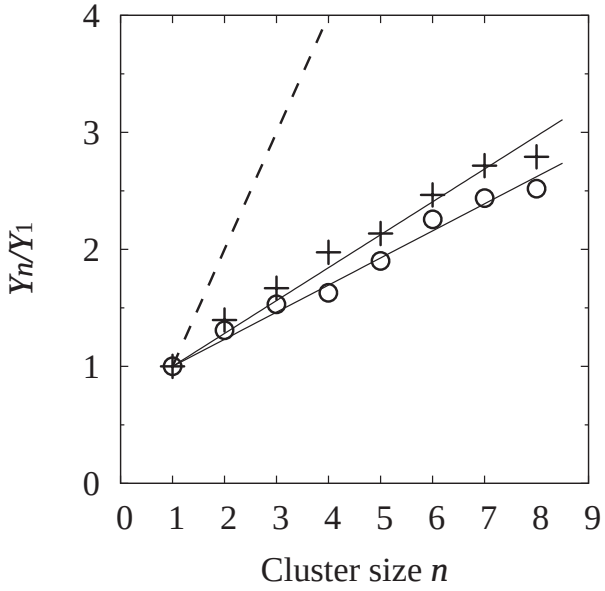

Fig. 4. Y_n/Y_1 values for impact of 12.5 keV/u C_n^+ on HOPG and KCl targets. Circles and crosses show the yields for KCl and HOPG, respectively. The solid lines were drawn to determine the slope α, while the dashed line represents $Y_n/Y_1 = n$, i.e., absence of the vicinage effect.

density around the trajectory in the target, and electron density oscillates typically with the plasma frequency of the target material.[14] This generates an oscillatory electric potential (the so-called *wake* potential) typical of a conductor material. For insulator targets such as KCl, an electric potential can also be generated. In this case, the role of free electrons in conductors will be played partly by ionized target electrons.

Strictly speaking, ion-induced electron emission suffers inherently from the disturbance due to the electric potential generated by the ion itself. For clusters, electric potential gives rise to further disturbance in the transport of electrons produced by other cluster atoms. The latter disturbance is a meaningful process only when the excitation range $b_{\rm m}$, which is the maximum impact parameter for the effective ionization of target electrons, is less than the interatomic spacing of the cluster. In the present case, $b_{\rm m} < 1$Å,[6] so that the condition is satisfied.

The effect of the above-mentioned disturbance is estimated from the interaction range of electric potential, R. A simple measure of R is given by

$$R = 2\pi V/\omega_{\rm p} \,, \tag{2}$$

where V is the ion velocity and $\omega_{\rm p}$ is the plasma angular frequency. For HOPG, for example, the estimated values of R, using $\hbar\omega_{\rm p} = 25\,$eV for carbon,[15] are 2.6 and 4.7 Å for 12.5 and 41.7 keV/u, respectively. It is realistic to regard R as an underestimated measure of the interaction range (corresponding to only one oscillation period). We may therefore expect

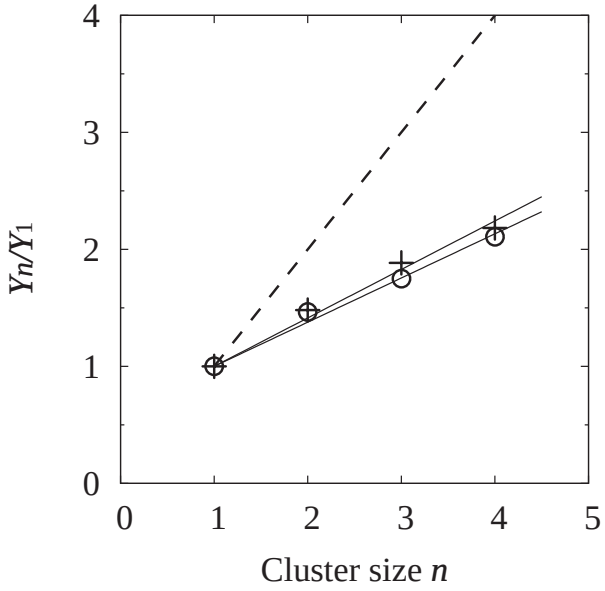

Fig. 5. Y_n/Y_1 for impact of 41.7 keV/u C_n^+ on HOPG and KCl targets. Circles and crosses show the yields for KCl and HOPG, respectively. The solid lines were drawn to determine the slope α, while the dashed line represents $Y_n/Y_1 = n$, i.e., the absence of the vicinage effect.

from the above values of R that electric potential affects the electrons at a distance of up to the order of 10 Å in the downstream space of the ion. Such a long-range interaction is consistent with the suppressed electron emission at 0° from a thick carbon foil.[7] In this case, the mean spacing between the cluster atoms estimated from Coulomb explosion is ∼10 Å for 41.7 keV/u $C_n^+(n \leq 4)$ passing through a C foil of ∼900 Å (20.3 μg/cm^2) thickness.

The electrons scattered by one of the constituent atoms therefore have a chance of experiencing the electric potential generated by the other atoms. Actually, the interaction ranges estimated above are longer than the interatomic spacing 1.3 Å of C_n^+, which increases with the Coulomb explosion and multiple scattering as the cluster penetrates the target. According to the calculations by Echenique et al.,[15] the amplitude of oscillatory electric potential in a carbon target is ∼10 eV behind the carbon ion in the present velocity range, assuming the effective charge state of $C^{q+}(q \simeq 1)$.[16] Clearly, such a potential field is enough to disturb the transport of low-energy electrons (less than ∼10 eV), which is predominant in the energy distribution of emitted electrons.

3.3 Geometrical estimate of α

At present, the quantitative treatment of suppressed electron emission in terms of electric potential seems to require complex calculations. However, the unique parameter α is not very sensitive to the experimental parameters such as the species of the cluster atom (including the cluster structure), projectile velocity, the type of target material, and measured direction. This

Table I. Values of α obtained from the present and published experimental data. The notations F and B represent the forward and backward measurements of the emitted electrons, respectively.

Projectile	Target: meas. direction	α	References
12.5 keV/u C_n^+	KCl: 180°	0.22±0.01	present work
41.7 keV/u C_n^+	KCl: 180°	0.36±0.03	present work
12.5 keV/u C_n^+	HOPG: 180°	0.26±0.01	present work
41.7 keV/u C_n^+	HOPG: 180°	0.40±0.03	present work
41.7 keV/u C_n^+	∼140Å C foil: 0°	∼0.15	Tomita et al.[7]
41.7 keV/u C_n^+	thick C foil: 0°	∼0.30	Tomita et al.[7]
20.0 keV/u C_n^+	HOPG, Si: 180°	∼0.30	Kudo et al.[6]
8.89 keV/u Al_n^+	HOPG: 180°	0.33±0.01	Kudo et al.[6]
8.89 keV/u Al_n^+	Si: 180°	0.40±0.01	Kudo et al.[6]
0.76 keV/u Au_n^+	140Å C foil: F	0.63±0.01	Fallavier et al.[12]
0.76 keV/u Au_n^+	thick C foil: F	0.80±0.02	Fallavier et al.[12]
40 keV/u H_n^+	C foil: B	0.49±0.02	Billebaud et al.[13]
80 keV/u H_n^+	C foil: B	0.71±0.03	Billebaud et al.[13]
40 keV/u H_n^+	C foil: F	0.53±0.03	Billebaud et al.[13]
80 keV/u H_n^+	C foil: F	0.63±0.03	Billebaud et al.[13]
30 keV/u H_n^+	∼200Å C foil: F+B	0.27±0.02	de Castro Faria et al.[11]
60 keV/u H_n^+	∼200Å C foil: F+B	0.33±0.02	de Castro Faria et al.[11]
80 keV/u H_n^+	∼200Å C foil: F+B	0.40±0.02	de Castro Faria et al.[11]
100 keV/u H_n^+	∼200Å C foil: F+B	0.54±0.02	de Castro Faria et al.[11]

implies the existence of a simple mechanism underlying electron suppression in the velocity range of clusters in Table I. Therefore, it is important to estimate a reasonable α even by crude considerations of the dicluster case ($n = 2$).

Ionized electrons with velocities slower than the projectile are discussed first. The effect of the generated electric field should depend on the orientation of the pair of cluster atoms (ions). In the aligned case in which the molecular axis is parallel to the running direction, the slow electrons ionized by the leading ion can be seriously scattered by the electric field of the trailing ion, while the electrons ionized by the trailing ion are unaffected by the electric field of the leading ion. Y_2/Y_1 in this case is roughly estimated as $1 + 0 = 1$. In contrast, there is no vicinage effect when the molecular axis is perpendicular to the running direction, i.e., $Y_2/Y_1 = 2$. At an angle θ between the molecular axis and the running direction, the reduction factor $f(\theta)$ for the trailing ion is assumed to be $f = \cos\theta$. By averaging f over all

the orientation, we may expect that

$$Y_2/Y_1 = 1 + \frac{1}{2\pi}\int_0^{\pi/2} f(\theta)\ 2\pi \sin\theta \,\mathrm{d}\theta = 1.5\ . \tag{3}$$

The above considerations can also be applied to the suppressed emission of electrons at 0° with velocities higher than the ion velocity.[7] In the aligned case ($\theta = 0°$), the roles of the leading and trailing ions noted above are interchanged. Indeed, the fast electrons induced by the leading ion do not encounter the electric field generated by the trailing ion, whereas those induced by the trailing ion suffer from the electric field generated by the leading ion.

Consequently, for the emission of both slow and fast electrons, we have an estimated value of $\alpha = 0.5$, from eqs. (1) and (3), which roughly reproduces the observations ($0.3 < \alpha < 0.7$) listed in Table I.

3.4 Possible shift of suppressed emission to enhanced emission

The electric potential generated by a moving charged particle can be discussed in terms of a linear dielectric response.[14] It is also applicable to the case of cluster ions, for which the vicinage effect for the dicluster case is briefly described to investigate the possible shift of suppressed emission to enhanced emission at high velocities.

We consider a dicluster of the velocity $\boldsymbol{V}$ and the effective point charge Ze per atom, located at $\boldsymbol{r} = \boldsymbol{V}t$ and $\boldsymbol{r} = \boldsymbol{V}t + \boldsymbol{s}$ in the target, with $\boldsymbol{s}$ being the relative position vector of the neighboring atom. In this case, the external charge density in the target material is given by

$$\rho_{\mathrm{ext}}(\boldsymbol{r}, t) = Ze\left[\delta(\boldsymbol{r} - \boldsymbol{V}t) + \delta(\boldsymbol{r} - \boldsymbol{V}t - \boldsymbol{s})\right] , \tag{4}$$

where δ represents the delta function for three-dimensional space. The electric potential due to the external charge plus polarized electrons is written using the dielectric function of the target material $\varepsilon(\boldsymbol{k}, \omega)$. Actually, it is given by

$$\phi(\boldsymbol{r}, t) = \frac{Ze}{(2\pi)^3}\int_0^{\infty}\left(1 + \frac{\sin ks}{ks}\right)\frac{\exp\left[\mathrm{i}\boldsymbol{k}(\boldsymbol{r} - \boldsymbol{V}t)\right]}{\varepsilon(\boldsymbol{k}, \boldsymbol{k}\boldsymbol{V})}\frac{\mathrm{d}^3k}{k^2}\ , \tag{5}$$

where $(\sin ks)/ks$ is the interference term arising from the neighboring atom, which is obtained by averaging over all directions of the molecular axis. In expressions more sophisticated than eq.(5),[3,4] the interference term also appears similarly to that in eq. (5).

The V dependence of the behavior of the interference term in eq. (5) is of primary interest. Equation (5) indicates that the neighboring atom enhances or reduces $\phi(\boldsymbol{r}, t)$ at a space around the cluster if the integral of the second term (proportional to the interference term) has a sign the same as or opposite sign to that of the first term, respectively. The sign of plus or minus should depend on the parameter V, similarly to the cluster stopping power which is given by the slope of $\phi(\boldsymbol{r}, t)$ at $\boldsymbol{r} = \boldsymbol{V}t$. Indeed, a shift of reduced stopping power to enhanced stopping power occurs for carbon clusters as the cluster speed reaches 2.0–2.5 times the Bohr velocity,

according to the calculations by Kaneko.[4] The enhanced $\phi(\boldsymbol{r}, t)$ causes enhanced disturbance of electron transport, leading to suppressed emission, corresponding to that in the case listed in Table I, while the reduced $\phi(\boldsymbol{r}, t)$ should lead to enhanced electron emission.

Thus far, the shift of suppressed emission to enhanced emission as cluster speed increases is recognizable only for H_2^+ and H_3^+, for which an enhanced emission occurs at energies (velocities) greater than $\sim$200 keV/u.[5,17] However, an electric potential will be only weakly generated at velocities in the Bethe stopping region, i.e., at energies higher than $\sim$100 keV/u. Therefore, the applicability of the present model to the enhanced electron emission observed for H_2^+ and H_3^+ requires more careful studies.

4. Conclusions

From the analysis of the linear n dependence of electron yield, the main factor for the suppression of cluster-induced electron emission has been deduced. Evidently, the suppression is predominantly caused by the disturbance of the electron escape made possible by the electric potential generated by moving cluster atoms.

The model accounts for the observed long-range interaction of dissociated cluster atoms. Also, a measure of the suppression effect, which is given by the slope of the linear n dependence of electron yield, has been reproduced roughly from the geometrical consideration of the generated electric field. Note that the track potential induced in KCl does not contribute to suppressed electron emission.

There is a possibility that the interference term in eq. (5) gives rise to a shift from suppressed emission to enhanced emission of electrons as cluster speed increases, corresponding to that in the case of cluster stopping power. However, the applicability of the present model to enhanced electron emission for fast clusters in a Bethe stopping region requires careful studies.

Acknowledgements

We thank staff members of UTTAC for technical assistance in the experiments, and Prof. T. Kaneko (Okayama University of Science) for valuable comments on this work.

References

1) D. Hasselkamp, H. Rotherd, K.-O. Groeneveld, J. Kemmler, P. Varga, and H. Winter: *Particle Induced Electron Emission II* (Springer, Berlin, Heidelberg, 1991).
2) W. Brandt, A. Ratkowski, and R. H. Ritchie: Phys. Rev. Lett. **33** (1974) 1325.
3) N. R. Arista: Phys. Rev. B **18** (1978) 1.
4) T. Kaneko: Phys. Rev. A **66** (2002) 052901.
5) See, for example, a review by M. Fallavier: Nucl. Instr. and Meth. B **112** (1996) 72.
6) H. Kudo, W. Iwazaki, R. Uchiyama, S. Tomita, K. Shima, K. Sasa, S. Ishii, K. Narumi, H. Naramoto, Y. Satoh, S. Yamamoto, and T. Kaneko: Jpn. J. Appl. Phys. **45** (2006) L565.
7) S. Tomita, S. Yoda, R. Uchiyama, S. Ishii, K. Sasa, T. Kaneko, and H. Kudo: Phys. Rev. A **73** (2006) 060901(R).
8) K. Kimura, S. Usui, K. Maeda, and K. Nakajima: Nucl. Instr. and Meth. B **193** (2002) 661.
9) K. Kimura, S. Usui, T. Tsujioka, S. Tanaka, K. Nakajima, and M. Suzuki: Vacuum **73** (2004) 59.
10) W. König, K. H. Krebs, and S. Rogaschewski: Int. J. Mass Spectrom. Ion Phys. **16** (1975) 243.
11) N. V. de Castro Faria, B. Farizon Mazuy, M. Farizon, M. J. Gaillard, G. Jalbert, S. Ouaskit, A. Clouvas, and A. Katsanos: Phys. Rev. A **46** (1992) R3594.
12) M. Fallavier, R. Kirsch, J. C. Poizat, J. Remillieux, and J. P. Thomas: Nucl. Instr. and Meth. B **164–165** (2000) 920.
13) A. Billebaud, D. Dauvergne, M. Fallavier, R. Kirsch, J. C. Poizat, J. Remillieux, H. Rothard, and J. P. Thomas: Nucl. Instr. and Meth. B **112** (1996) 79.
14) J. Lindhard: Mat. Fys. Medd. Dan. Vid. Selsk. **28**, (1954) No. 8, 1.
15) P. M. Echenique, R. H. Ritchie, and W. Brandt: Phys. Rev. B **20** (1979) 2567.
16) K. Shima, N. Kuno, and M. Yamanouchi: Phys. Rev. A **40** (1989) 3557.
17) D. Hasselkamp: Phys. Stat. Solidi A **79** (1983) K197.